

MOTIVATION

The Midlatitude Continental Convective Clouds Experiment (MC3E) was conducted April-June 2011 with instrumentation concentrated within the ARM Southern Great Plains site near Lamont, Oklahoma (Fig. 1). Included within this suite of instruments were three ARM X-band polarimetric radars (XSAPRs), one ARM C-band polarimetric radar (CSAPR), and a NASA S-band polarimetric radar (NPOL). This setup provided the opportunity for multiple Doppler synthesis, as well as a means for data comparison, including validation from observations at the Central Facility. Our initial focus has been on quality control of the radar data, specifically at shorter wavelengths where attenuation is a major issue, in order to provide a reliable dataset for creating products in support of ASR modeling efforts. In addition to being able to determine vertical velocities, the availability of the radar data at multiple frequencies will allow for improvements in rainfall estimation and hydrometeor identification. For polarimetric-based rainfall estimation, the XSAPR data will be particularly useful at lighter rain rates due to the greater sensitivity to phase shifts at X-band. Also due to this increased sensitivity, Dolan and Rutledge (2009) demonstrated improved identification of ice crystals, which will be particularly important when extending our ASR work to winter systems.



Fig. 1. ARM Southern Great Plains site during MC3E.

HYDROMETEOR IDENTIFICATION

Hydrometeor identification at X-band is based on the methodology of Dolan and Rutledge (2009), with the addition of three new species for summer precipitation: wet snow, hail, and big drops. Range of values and corresponding membership functions were determined from scattering simulations and are a continuing work in progress, along with developing an algorithm specific to winter systems.

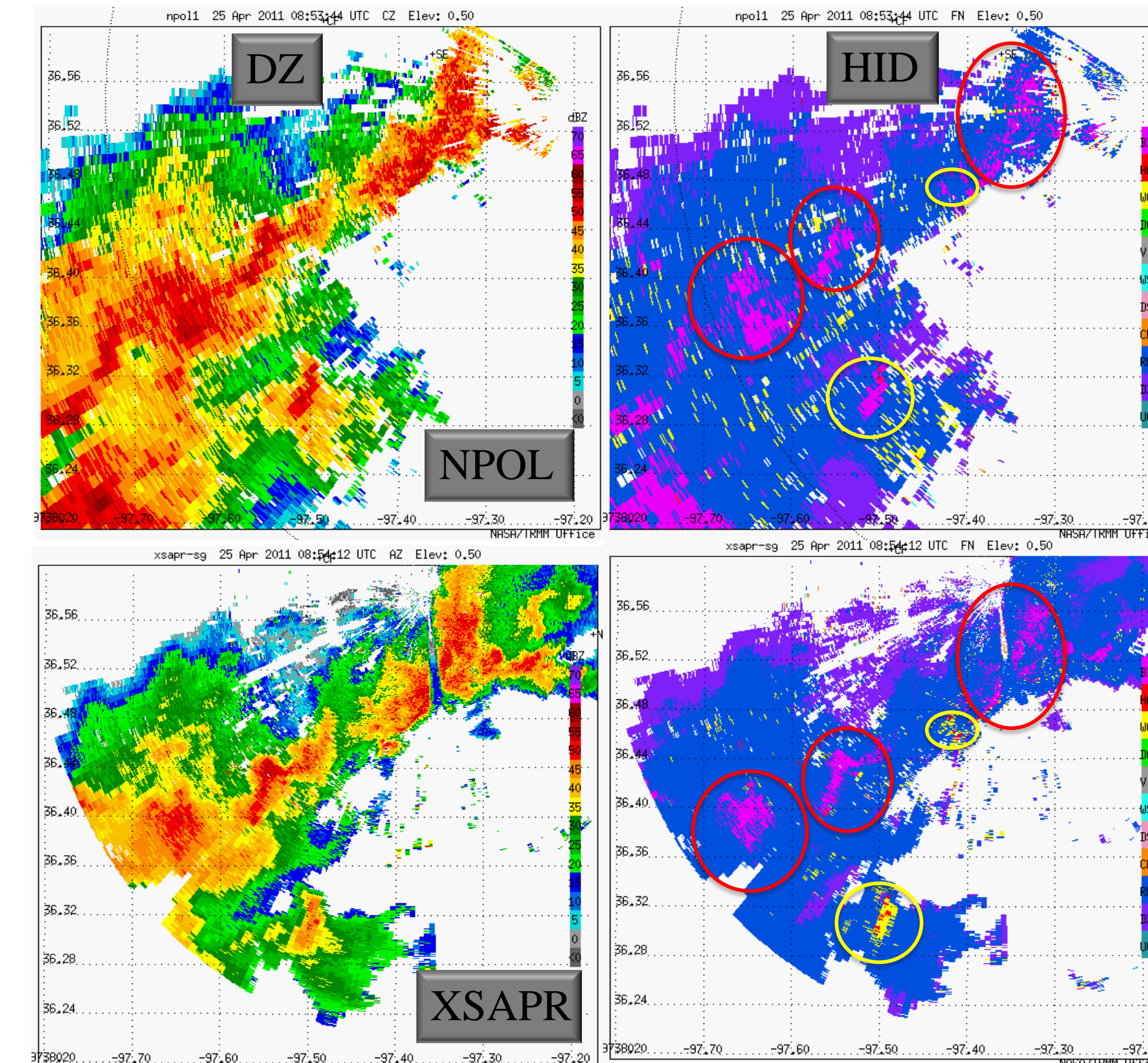


Fig. 3. Comparison between NPOL (top) and XSAPR (SE, bottom) for reflectivity (left) and HID (right) at 0849 UTC on 25 April 2011.

XSAPR reflectivity looks low compared to NPOL (Fig. 3, left), as previously shown, but HID at these low levels (Fig. 3, right) shows generally good agreement with coincident areas of rain (blue), and big drops (pink, red circles). However, XSAPR HID identifies regions of graupel and hail (yellow circles) where NPOL sees liquid hydrometeors. An HID, tuned for C-band, was also applied to CSAPR, showing similar results, but needs further work due to issues with Z_{DR} . Issues with over identification of high density graupel at all wavelengths is being investigated.

PARTITIONING AND VERTICAL VELOCITY

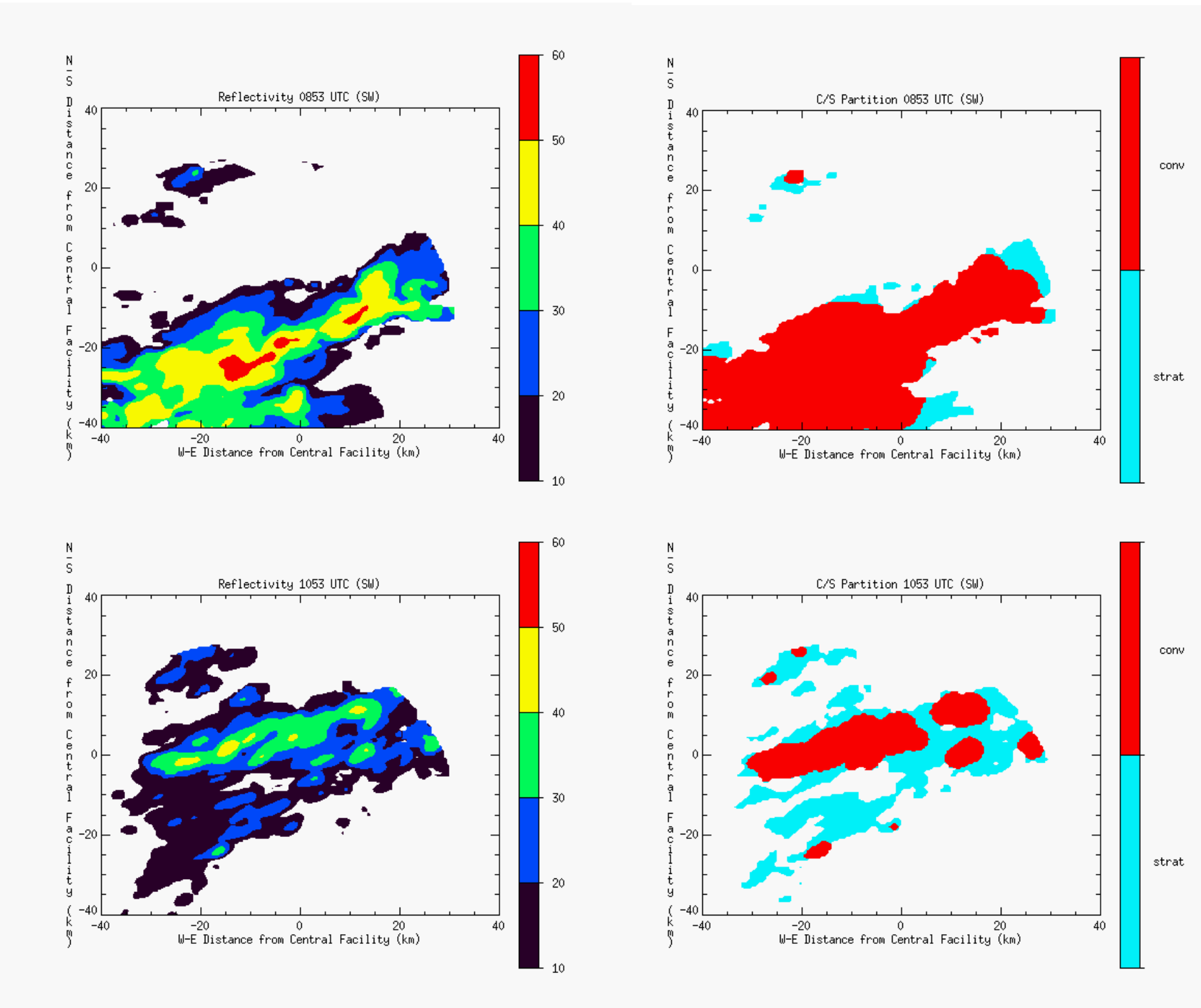


Fig. 6. PPIs at 1 km of XSAPR (SW) reflectivity (left) and the corresponding convective/stratiform partitioning (right) for 0853 UTC (top) and 1053 UTC (bottom) on 25 April 2011.

A convective/stratiform partitioning algorithm was applied following Steiner et al. (1995) and Yuter and Houze (1997, 1998). As can be seen from two examples in Fig. 6, one at 0853 UTC (top) and another later at 1053 UTC (bottom) on 25 April 2011, the partitioning does a reasonable job isolating the convective areas. Although this was not a classic leading convection/trailing stratiform case, weaker precipitation appears to be correctly classified as stratiform.

CFADs of radar reflectivity provide a means to evaluate data from the entire volume. This also allows for the evolution of the system as a whole to be investigated, as is seen in the example in Fig. 7, highlighting an overall weakening of convection between the two times shown (Fig. 7a,b). In addition, dual-Doppler analyses (between the SE and SW XSAPRs) and the partitioning algorithm provides information on mean vertical velocities, for example, in the convective and stratiform regions. A convective updraft is evident at 0853 UTC (Fig. 7c), followed by a decline in upward velocities by 1053 UTC (Fig. 7d), with the stratiform area exhibiting weak downward (upward) motion at lower (upper) levels.

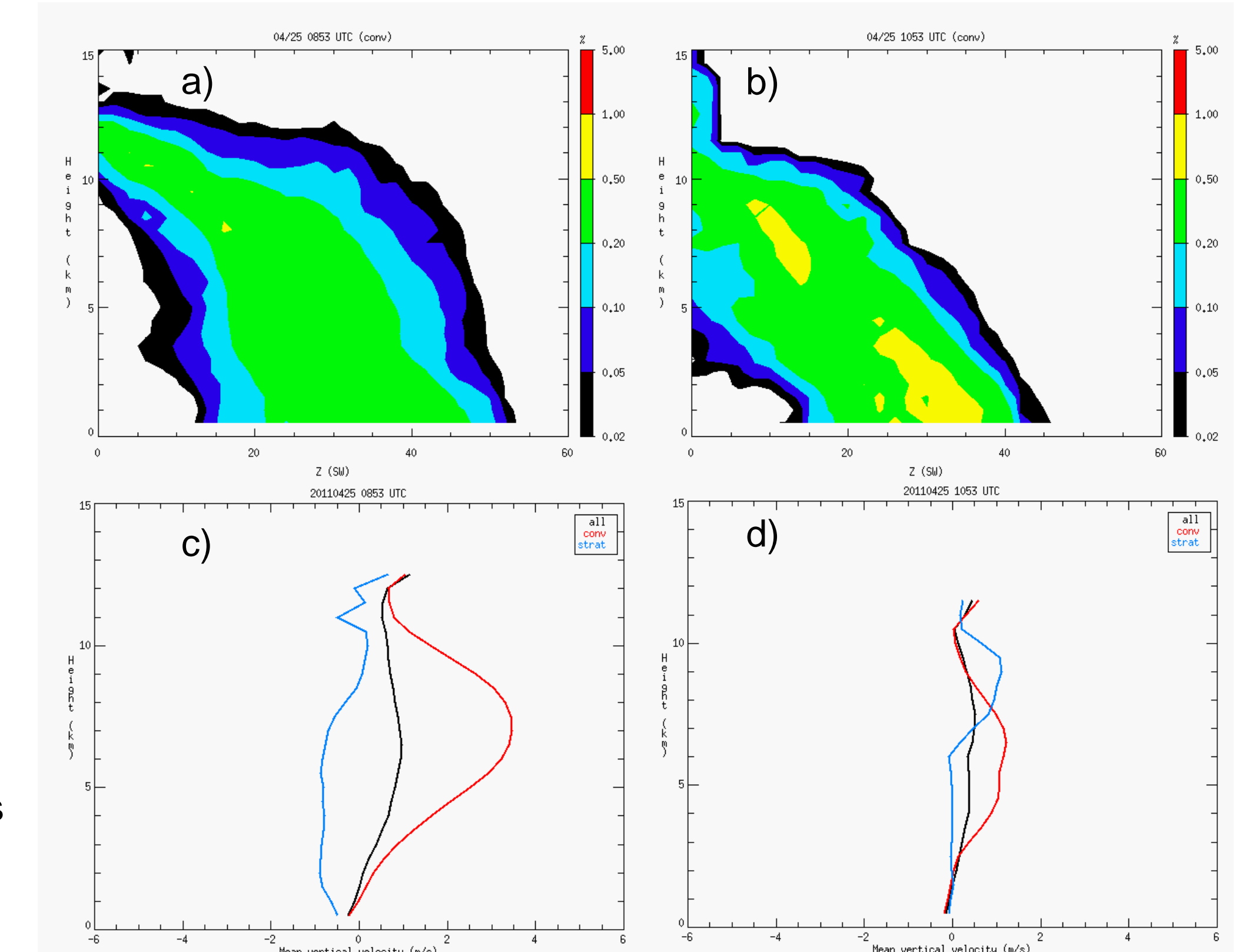


Fig. 7. Contoured frequency by altitude diagrams (CFADs) of XSAPR (SW) reflectivity (a,b) for convective points only and mean profiles of partitioned vertical velocity (c,d) for 0853 UTC (a,c) and 1053 UTC (b,d) on 25 April 2011.

QUALITY CONTROL (XSAPRs)

- Unfolding phase (SE)
- Unfolded radial velocities by hand (Nyquist velocities of 16.8 ms^{-1} (SE) and 17.2 ms^{-1} (SW) resulting in multiple folds)
- Z_{DR} bias from vertically pointing data: -3.6 dB (SW) and $+0.1 \text{ dB}$ (SE)
- Removal of non-meteorological echo
- -1^{st} pass removed echo where $\rho_{HV} < 0.7$ below 2.5 km and where $SQ < 0.5$
- -2^{nd} pass removed echo where $\rho_{HV} < 0.4$ and $SD(\Phi_{DP}) < 60^\circ$ (to retain brightband)
- Filtered Φ_{DP} , but used K_{DP} from the raw files (via Wang and Chandrasekar 2009)

- Phase-based attenuation correction from Carey et al. (2000), adapted for X-band:

$$Z(\text{corrected}) = Z(\text{uncorrected}) + a(\text{filtered phase} - \text{offset phase})$$

$$Z_{DR}(\text{corrected}) = Z_{DR}(\text{uncorrected}) + b(\text{filtered phase} - \text{offset phase})$$

- Coefficients (a and b) empirically estimated at each time by the slope of the best-fit line for filtered phase vs. Z and Z_{DR} , respectively, in rain-only regions.
- Estimated offset phase: 100° (SW) and 300° (SE)

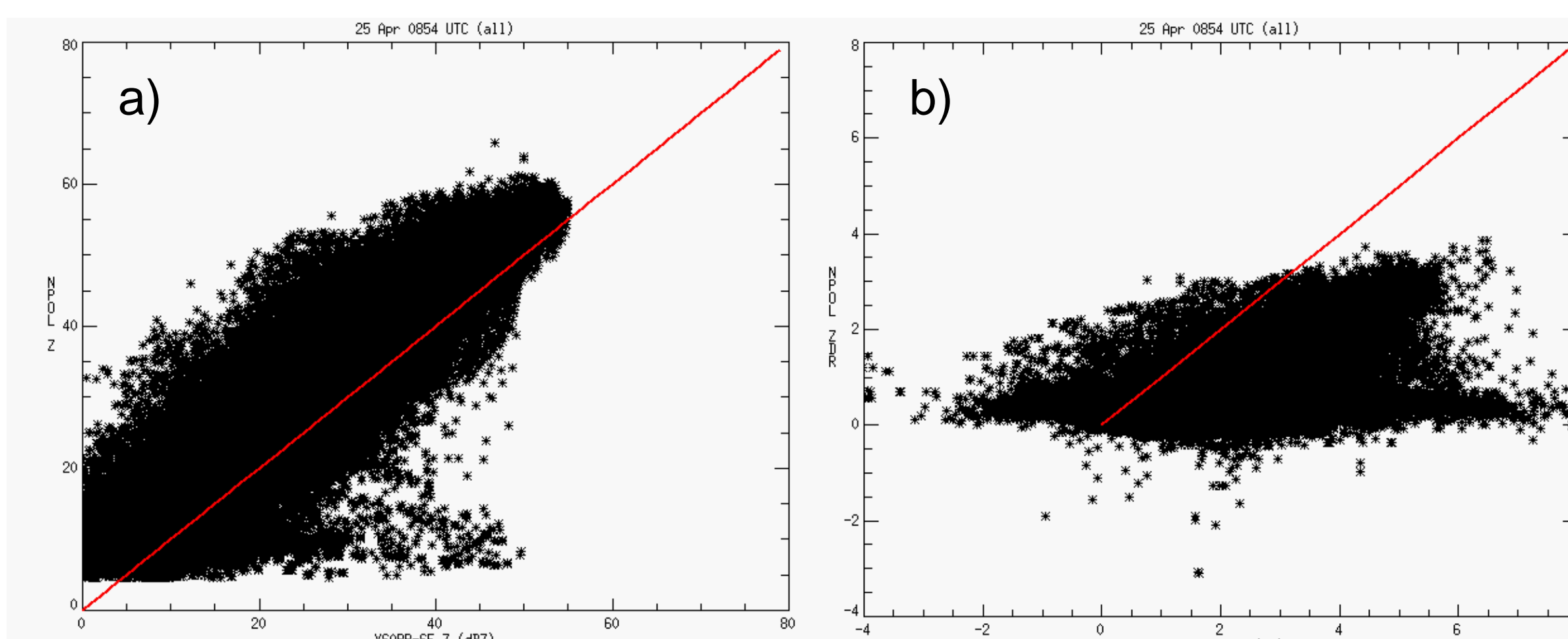


Fig. 2. Comparisons between XSAPR (x-axis) a) reflectivity with NPOL Z, b) Z_{DR} with NPOL Z_{DR} , and c) Z with disdrometer data on 25 April 2011.

- Comparison with NPOL (Fig. 2a,b) suggests XSAPR Z (Z_{DR}) under (over) corrected

- Comparison with five NASA 2DVDs (Fig. 2c) also suggests an under correction of XSAPR Z

Vertical profiles of HID species show generally good agreement between both radars, with hydrometeor species peaking at the same heights. NPOL generally shows more aggregates (Fig. 4a, AG, red), while XSAPR identifies larger percentages of ice crystals (Fig. 4a, CR, green), consistent with the increased sensitivity to phase shifts at X-band. Another promising feature is the identification of big drops at X-band (Fig. 4b, BD, red).

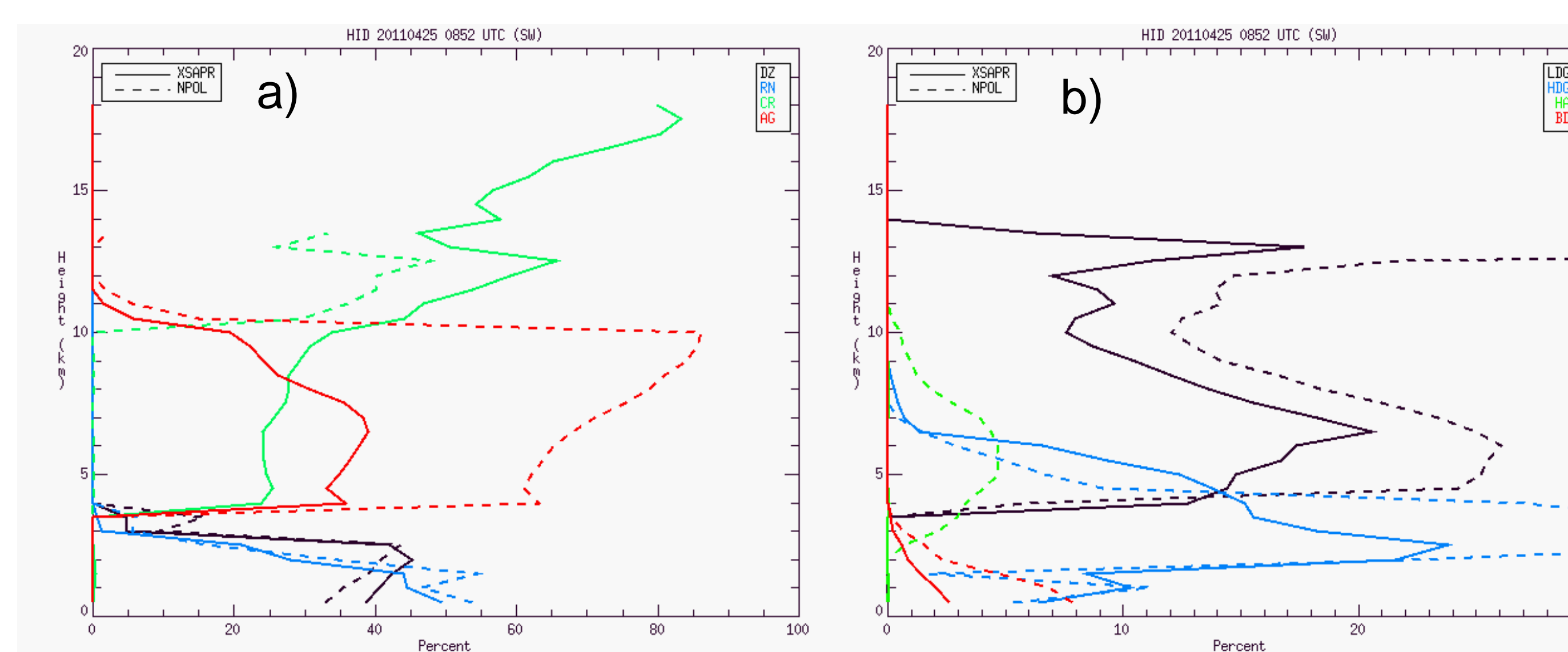


Fig. 4. Vertical profiles of percentage of HID species at 0852 UTC on 25 April 2011 for XSAPR (SW, solid lines) and NPOL (dashed lines)

The horizon-to-horizon RHIs provide another unique opportunity to evaluate the vertical distribution of hydrometeors within storms. The example in Fig. 5 highlights widespread stratiform precipitation with embedded convective elements. The melting level (near 3.5 km on this day) is characterized by a reflectivity brightband (Fig. 5, top) and wet snow (Fig. 5, bottom, WS, light blue). Above this area, ice crystals (CR, orange), dry snow (DS, pink), and vertically aligned ice (VI, gray) are identified, with drizzle (DZ, purple) and rain (RN, dark blue) below. Small areas of graupel (DG, green; WG, yellow) are also observed within the convective areas, demonstrating promising results.

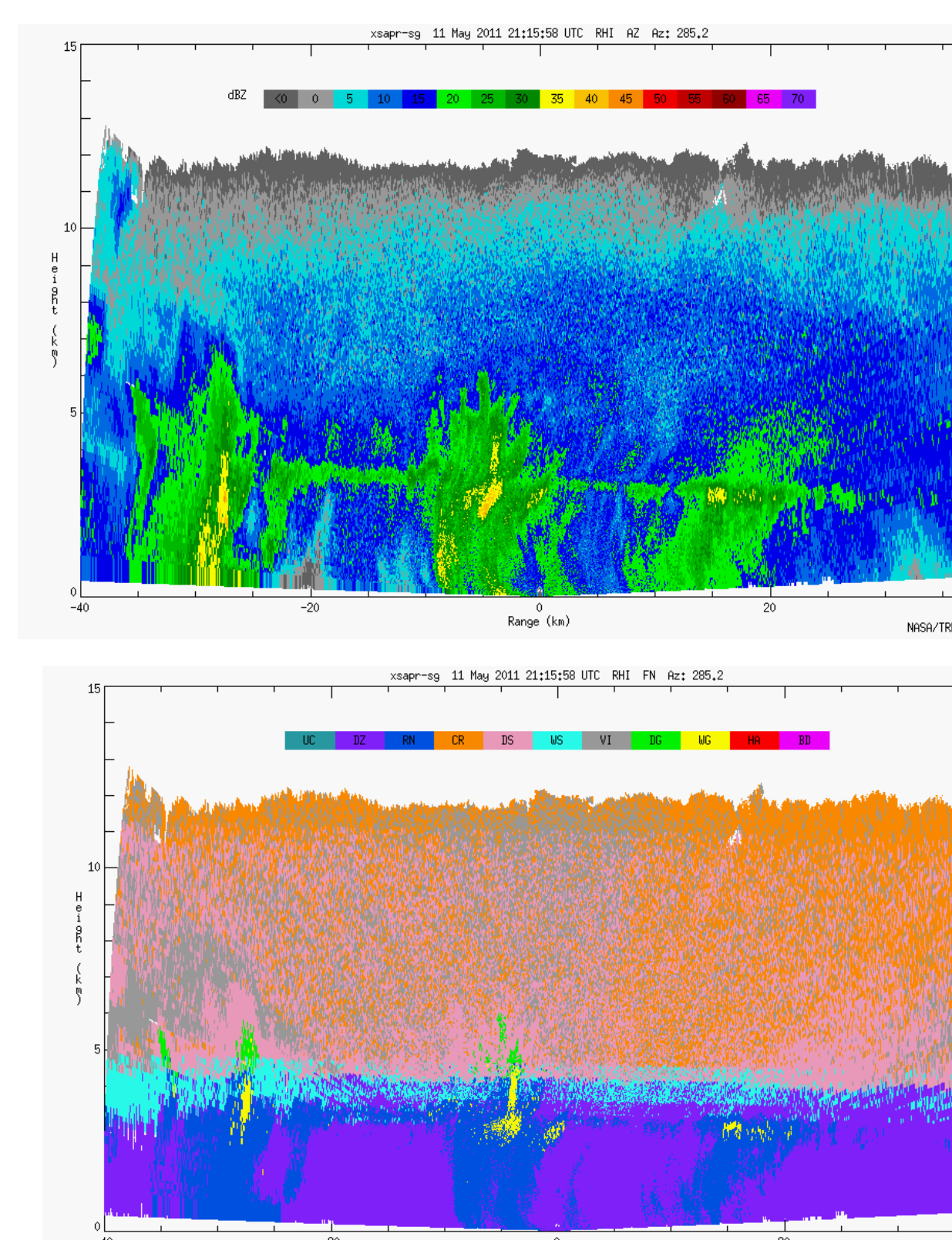


Fig. 5. Horizon-to-horizon XSAPR RHI at 2115 UTC on 11 May 2011 for reflectivity (top) and HID (bottom).

FUTURE WORK

We have highlighted the initial work using the XSAPR data from MC3E, focusing primarily on quality control of the data and moving forward with some preliminary results regarding vertical velocities and hydrometeor identification. As we continue to improve upon the attenuation correction for the XSAPR data, we will also aid in efforts to correct CSAPR data. We are working on adding the CSAPR data to our analysis in the effort to produce dual-wavelength HID and rainfall estimation. Including CSAPR data will also improve vertical velocity results through multiple Doppler syntheses. As we continue to extend this analysis to additional cases from MC3E, we also plan to investigate winter cases, where the utility of increased phase shifts at X-band will prove increasingly useful for identification of frozen hydrometeors.

ACKNOWLEDGEMENTS

This research was supported by the Office of Science (BER), U.S. Department of Energy. Contact Info: Angela Rowe, CSU Atmospheric Science, Fort Collins, CO, arowe@atmos.colostate.edu